Cell detection and counting through cell lysate impedance spectroscopy in microfluidic devices†

Xuanhong Cheng,[a] Yi-shao Liu,[b] Daniel Irimia,[a] Utkan Demirci,[a] Liju Yang,[bc] Lee Zamir,[de] William R. Rodríguez,*[de] Mehmet Toner*[a] and Rashid Bashir*[b]

Received 3rd April 2007, Accepted 17th April 2007
First published as an Advance Article on the web 11th May 2007
DOI: 10.1039/b705082h

Cell-based microfluidic devices have attracted interest for a wide range of applications. While optical cell counting and flow cytometry-type devices have been reported extensively, sensitive and efficient non-optical methods to detect and quantify cells attached over large surface areas within microdevices are generally lacking. We describe an electrical method for counting cells based on the measurement of changes in conductivity of the surrounding medium due to ions released from surface-immobilized cells within a microfluidic channel. Immobilized cells are lysed using a low conductivity, hypotonic media and the resulting change in impedance is measured using surface patterned electrodes to detect and quantify the number of cells. We found that the bulk solution conductance increases linearly with the number of isolated cells contributing to solution ion concentration. The method of cell lysate impedance spectroscopy is sensitive enough to detect 20 cells μL^{-1}, and offers a simple and efficient method for detecting and enumerating cells within microfluidic devices for many applications including measurement of CD4 cell counts in HIV patients in resource-limited settings. To our knowledge, this is the most sensitive approach using non-optical setups to enumerate immobilized cells. The microfluidic device, capable of isolating specific cell types from a complex bio-fluidic and quantifying cell number, can serve as a single use cartridge for a hand-held instrument to provide simple, fast and affordable cell counting in point-of-care settings.

Introduction

Microfluidic systems have shown unique promise for studying cell function,[1–3] cell and tissue engineering,[4,5] disease diagnosis,[6–8] blood sample preparation,[9] and drug discovery.[10] Very recently, the use of microfluidics to isolate pure populations of leukocyte subsets from whole blood has attracted a lot of interest for point-of-care diagnostics.[8] As a specific example, 100 to 10 000 CD4+ T lymphocytes were captured from 10 μL of whole blood on the surface of a microdevice with a footprint of 2 cm^2. These cells were counted afterwards manually, using an optical microscope to monitor HIV infected patients. While the principle behind this cell isolation approach can be easily adapted to a wide spectrum of clinical applications, detecting these isolated cells remains a technical challenge to be addressed.

The use of optical microscopy for detection and quantification of surface immobilized cells within microdevices does not represent the optimal solution for point-of-care applications. This is because optical detection methods depend on a stable light path, lensing, filtering, and focusing mechanisms that could add cost and complexity to detection. In addition, optical detection tends to be low throughput, due to the small detection area available at a single time. At the same time, the most commonly used cell counting strategies, like flow cytometry[11,12] and impedance measurement (*i.e.*, Coulter counters),[13] can not be applied to cells attached on surfaces, despite miniaturized platforms that have been implemented by several researchers.[11,13–15] Alternative techniques to detect attached cells by substrate impedance sensing require cell coverage on the electrode surface to reach near unity for detectable measurements.[16–18] Studies using non-optical methods to detect few cells on large surface areas in a relatively large volume—including even the microlitre volumes of microscale devices—have not yet been reported, despite the need for non-optical detection methods in microfluidic applications.

To address the need to sensitively detect a small number of cells immobilized on a relatively large surface area or in a large

[a]*BioMEMS Resource Center and Center for Engineering in Medicine, Massachusetts General Hospital, Harvard Medical School, and Shriners Hospital for Children, Boston, Massachusetts 02114, USA. E-mail: mtoner@sbi.org; Fax: +1-617-724-2999; Tel: +1-617-371-4876*
[b]*Birck Nanotechnology Center, School of Electrical Engineering and Computer Engineering, Weldon School of Biomedical Engineering, Purdue University, West Lafayette, IN 47907, USA. E-mail: bashir@purdue.edu; Fax: +1-765-494-6441; Tel: +1-765-496-6229*
[c]*Now at Biomanufacturing Research Institute & Technology Enterprise (BRITE), Department of Chemistry, North Carolina Central University, Durham, NC 27707, USA*
[d]*Partners AIDS Research Center, Massachusetts General Hospital, 02114, USA. E-mail: wrodriguez@partners.org.; Fax: +1-617-726-4691; Tel: +1-617-726-8099*
[e]*Division of AIDS, Harvard Medical School, and Brigham and Women's Hospital, Boston, Massachusetts, 02115, USA. E-mail: wrodriguez@partners.org.; Fax: +1-617-726-4691; Tel: +1-617-726-8099*

† This paper is part of a special issue 'Cell and Tissue Engineering in Microsystems' with guest editors Sangeeta Bhatia (MIT) and Christopher Chen (University of Pennsylvania).

volume, we investigated the release of intracellular ions from lysed cells immobilized in a microfluidic channel, using surface-patterned electrodes to measure bulk conductance changes through impedance spectroscopy. Mammalian cells contain a significant amount of ions, and tight control of ion transport across cell membranes is central to normal cell function and response to the surrounding environment. When cells are suspended in hypotonic media, passive diffusion and active pumping of intracellular ions to the extracellular milieu are used to adjust to the hypo-osmotic environment. Here, we show that by controlled release of intracellular ions, we can perform impedance measurements to determine the number of cells present in a microfluidic channel. Using captured and immobilized CD4+ T cells as an example, following our previous success in separating these cells from whole blood, we demonstrate that cell lysate impedance spectroscopy has a detection threshold of 20 cells μL^{-1}, which is sufficiently useful for clinical and research applications.

Modeling of cell ion release-based impedance spectroscopy

Conductance *vs.* capacitance change due to ion release

When cells release ions, both bulk conductance and capacitance are affected. In a typical mammalian cell, cytoplasmic ion concentration is roughly 150 mM.[19] Given a volume of 0.2 pL, a typical lymphocyte, therefore, contains a total of 3×10^{-14} molar ions. After lysis in a 10 μL microchamber (the volume of the microfluidic device used in this study), these ions contribute to a 3 nM increase of ionic concentration. Thus, for every 100 lymphocytes, complete lysis in a 10 μL chamber would increase the solution ionic concentration by 0.3 μM. If we simplify the situation by assuming all released ions are potassium and chloride ions, and that potassium and sodium ions have comparable electrical mobility,[20] the solution conductivity can be calculated to increase by 0.03 $M\Omega^{-1}$ cm^{-1} from an increase of 0.3 μM in ionic concentration.[21] This conductivity change is more than 50% of the increase seen with deionized water (0.055 $M\Omega^{-1}$ cm^{-1}). In comparison, capacitance depends only weakly on ionic concentration in a dilute solution. For a sodium chloride solution, for example, the dielectric constant drops by only 10^{-7} for every nanomolar increase in ion concentration in a dilute solution (<100 mM).[22] Using a similar calculation, the total ions released from 100 lymphocytes only reduces the solution capacitance by 4×10^{-7} relative to deionized water (dielectric constant of 80). This change is several orders of magnitude lower than the change in bulk conductance. Thus, cell ion release mainly contributes to solution conductance change, which can be easily detected using impedance spectroscopy.

Modeling of impedance spectra

To understand solution conductance as a function of cell number, we carried out modeling studies to extract bulk conductance in microfluidic devices from impedance spectra obtained using surface patterned electrodes. Electrodes in an electrolyte solution can be modeled using an equivalent circuit as shown in Fig. 3a,[23,24] where C_{di} is the dielectric capacitance (it contains dielectric contributions from all the materials surrounding the electrodes, including the solution), R_{sol} is the bulk solution resistance (charge transport across the bulk solution), Z_{dl} is the interfacial impedance (the so-called Warburg impedance), which accounts for the change in the ionic gradient at the interface, and R_{ser} is the resistance of the on-chip wiring. The interfacial impedance can be expressed as

$$Z_{dl} = 1/[(j\omega)^n B] \quad (1)$$

Where $j = \sqrt{(-1)}$, n and B are parameters dependent on the properties of the electrolytes and of the electrodes. This is the simplest model that would properly fit the measured data over the whole frequency range at all times.

Materials and methods

Chemicals

Sucrose was purchased from Mallinckrodt Baker, Inc. (Paris, Kentucky, USA). Dextrose and Trypan blue solution (0.4%) was purchased from Sigma–Aldrich (St. Louis, MO, USA). Ficoll–Paque Plus was purchased from GE Healthcare Amersham Biosciences Corp (Piscataway, NJ, USA). 3-Mercaptopropyl trimethoxysilane was purchased from Gelest (Morrisville, PA, USA). Gold slides were obtained from Fisher Scientific (Fair Lawn, NJ, USA). Phosphate buffered saline (PBS) was obtained from Mediatech (Herndon, VA, USA). Lyophilized bovine serum albumin (BSA) was obtained from Aldrich Chemical Co. (Milwaukee, WI, USA). The coupling agents GMBS (*N*-γ-maleimidobutyryloxy succinimide ester) and NeutrAvidin were obtained from Pierce Biotechnology (Rockford, IL, USA). Biotinylated mouse anti-human anti-CD4 (clone 13b8.2) was purchased from Beckman Coulter (Somerset, NJ, USA).

Devices

Three types of devices were fabricated, implementing three different electrode designs, including interdigitated (IDT) co-planar electrodes, simple two-rail co-planar electrodes, and top- and bottom-electrodes (Fig. 1c–d). The gold electrodes were constructed using standard photolithography and gold wet etching processes. The IDT electrode fingers were 3.8 mm × 15 μm, with spacing of 35 μm. They covered the entire area within the microfluidic channel and were broken into three identical segments to probe different sections of the chamber. The connecting rails for the IDT electrodes and the rails of the simple two-rail electrodes were 100 μm wide with spacing of 3.8 mm. The top–bottom electrodes were 5 cm × 4 mm gold pads.

For all devices, the top and bottom slides (75 mm × 25 mm) were bonded to 50 μm thick PDMS gaskets with an opening of 5 cm × 4 mm, forming closed microfluidic channels. The PDMS gaskets were prepared by spin-coating PDMS on transparency slides, followed by hand-cutting windows of desired size. Two holes were drilled on the top glass and assembled with PDMS ports to form fluid inlets and outlets. Devices employed to measure impedance from off-chip lysates were used directly after assembly. Devices employed for cell

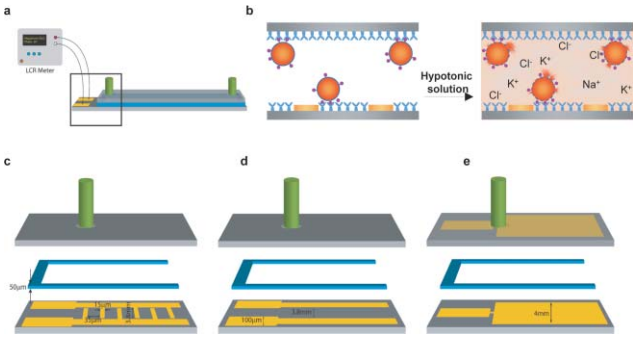

Fig. 1 Microfluidic devices and the experimental set up for impedance spectroscopy measurement. (a) Schematic drawing of the impedance measurement set up. Samples were delivered into the microchannels through an inlet (green) *via* a syringe pump, and impedance was measured using an LCR meter. (b) Illustration showing measurement of cell ion release using impedance spectroscopy. Target cells isolated within a microfluidic device are lysed to release intracellular ions. This leads to the increase of bulk conductance change, which can be monitored using surface patterned electrodes and impedance spectroscopy to detect cell numbers. Details of the electrode layout and device assembly are shown in (c)–(e): (c) interdigitated (IDT) co-planar electrodes, (d) simple two-rail co-planar electrodes and (e) top–bottom electrodes. The electrodes were patterned either on the bottom slides (for the IDT and two rail electrode designs) or on both slides (for the top–bottom electrode design) using standard cleanroom techniques and gold wet etching process. All devices were made by bonding two pieces of glass slide to 50 μm-thick PDMS gaskets (blue). Holes were drilled on the cover slides and assembled with PDMS ports to serve as sample inlets and outlets.

capture and on-chip lysis were functionalized with a monoclonal CD4 antibody and primed with PBS containing 1% BSA and 1 mM EDTA, as previously described.[8]

Cell preparation and on-chip cell isolation

Peripheral blood mononuclear cells (PBMCs) were prepared from freshly drawn blood through Ficoll density gradient centrifugation,[25,26] and maintained in RPMI-1640 medium. To isolate CD4+ T lymphocytes, PBMCs maintained in RPMI-1640 media were injected into anti-CD4 antibody functionalized microelectrode devices at a flow rate of 5 μL min^{-1} for different lengths of time, followed by rinsing of unbound cells from the devices using PBS containing 1% BSA and 1 mM EDTA. The number of cells captured within the microfluidic devices was counted manually under a phase contrast microscope.[8]

Off-chip sample preparation for impedance measurement

To prepare cell lysates off-chip, cultured PBMCs were counted manually using a hemocytometer, then diluted with RPMI-1640 to different concentrations ranging from 0 to 3500 cells μL^{-1} in eppendorf tubes, with a final volume of 1 mL. Afterwards, the cells were pelleted at 1200 g for 5 min and gently washed three times with 1 mL of low-conductive media (8.5% sucrose and 0.3% dextrose). After the final wash, the cells were resuspended in 1 mL of sterilized deionized water and left to sit at room temperature for 20 min for cell lysis. Each cell lysate was then injected into the microelectrode devices starting from the lowest concentration at a flow rate of 15 μL min^{-1}, and impedance spectra were taken after signals were stable. The devices were rinsed with deionized water between lysate injections at a flow rate of 50 μL min^{-1} until the impedance measurement reached the original values for deionized water.

Optical characterization of on-chip cell lysis using sugar solutions

To identify a low conductive media to lyse cells at a controlled rate, we diluted a low conductive viability-maintenance solution containing 8.5% sucrose and 0.3% dextrose to different final concentrations. These solutions were injected sequentially into microfluidic channels with captured CD4+ T lymphocytes using a syringe pump (Harvard Apparatus) at a flow rate of 15 μL min^{-1} for 1 min, and cells were allowed to lyse in each solution for 10 min. These cells were pre-stained using Fluo-3[27] and captured in microfluidic channels by surface-immobilized antibodies using methods described previously.[8] Fluorescent images were taken every 30 s throughout the course of the experiment and the number of fluorescent cells were enumerated to estimate the number of intact cells.

On-chip preparation for impedance spectroscopy

To detect surface immobilized cells, ions present in PBS buffer were washed out of the channels using a low conductivity washing solution containing 8.5% sucrose and 0.3% dextrose, at a flow rate of 20 μL min^{-1} until impedance signals were stable. Next, a low-conductive cell lysing solution containing 2% sucrose and 0.07% dextrose was flowed in at a flow rate of 10 μL min^{-1} for 1 min for cell lysis. After the lysing solution was introduced, flow was stopped and cells were kept in this solution for another 10 min to allow cell lysis to reach steady state. Following cell lysis, deionized water was injected at a flow rate of 20 μL min^{-1} for 5–10 min to acquire reference spectra. Impedance was monitored continuously throughout the entire process.

Impedance spectroscopy measurements

Impedance measurements were taken using an Agilent 4284 LCR meter (Agilent Technologies Inc., Palo Alto, CA, USA). The microelectrode devices were connected to the LCR meter through platinum probes; a schematic of the experimental setup is shown in Fig. 1a. The impedance measurement process was automated by custom LabView (National Instruments Corp., Austin, TX, USA) virtual instruments and GPIB interface. Impedance spectra were measured in the frequency range of 100 Hz to 1 MHz with a frequency increase factor of 1.5, and amplitude of 250 mV.

Results

All devices used in this study are composed of surface microelectrodes patterned within channels with the dimensions of 5 cm × 4 mm × 50 μm. When immobilized with a specific antibody and operated under controlled flow conditions, this channel design has been shown previously to specifically isolate CD4+ T lymphocytes (purity >95%) with high

efficiency (>90%) from unprocessed whole blood.[8] In the current study, we further functionalized antibodies in microchannels with patterned microelectrodes for the purpose of detecting isolated cells electrically. Using an appropriate electrode layout for on-chip cell lysis and counting (Fig. 1c), both isolation purity and yield remained above 90% for CD4+ T cell separation from whole blood, due to maintenance of 85% of affinity surface areas within the channels. Since cell isolation has been described in detail previously,[8] we focus on describing electrical detection of isolated cells in the current work.

Impedance measurement using off-chip cell lysate

To test the detection sensitivity of ion release from primary cells using impedance spectroscopy, we first lysed PBMCs of known concentrations in eppendorf tubes with deionized water, and measured impedance of the lysate using microfluidic devices of three different electrode designs: top–bottom electrodes, IDT co-planar electrodes and simple two-rail co-planar electrodes. Fig. 2a and b show the spectra of impedance magnitude and phase as a function of frequency for cell concentrations ranging from 0 to 3000 cells μL^{-1}, measured using the IDT electrodes. We observed that each magnitude spectrum has two regions, a constant impedance region in the frequency range from 100 Hz to 10 kHz, and a region of decreasing impedance at the higher frequency range (>100 kHz). With increasing cell concentrations, there is a consistent decrease in impedance magnitude in the low-frequency range, and a shift of the phase peak to a higher frequency. This suggests strongly that semi-quantitative measurement of cell concentrations can be determined using cell ion release. The impedance magnitude spectra obtained from the other two electrode designs demonstrated similar properties, but different absolute values; the impedance magnitude measured using two-rail electrodes are two orders of magnitude higher than those from the IDTs, which is another two orders of magnitude higher than the top–bottom electrodes. The transition point where impedance begins to drop on the magnitude spectra occurs around 10 kHz for the top–bottom electrodes, but shifted to around 1 kHz for the simple two-rail electrodes (data not shown).

To examine the ability of the impedance spectra to discriminate cell concentrations, we plotted impedance magnitude at 760 kHz *versus* cell concentration for the three types of electrode designs (Fig. 2c–e). We chose 760 kHz as the

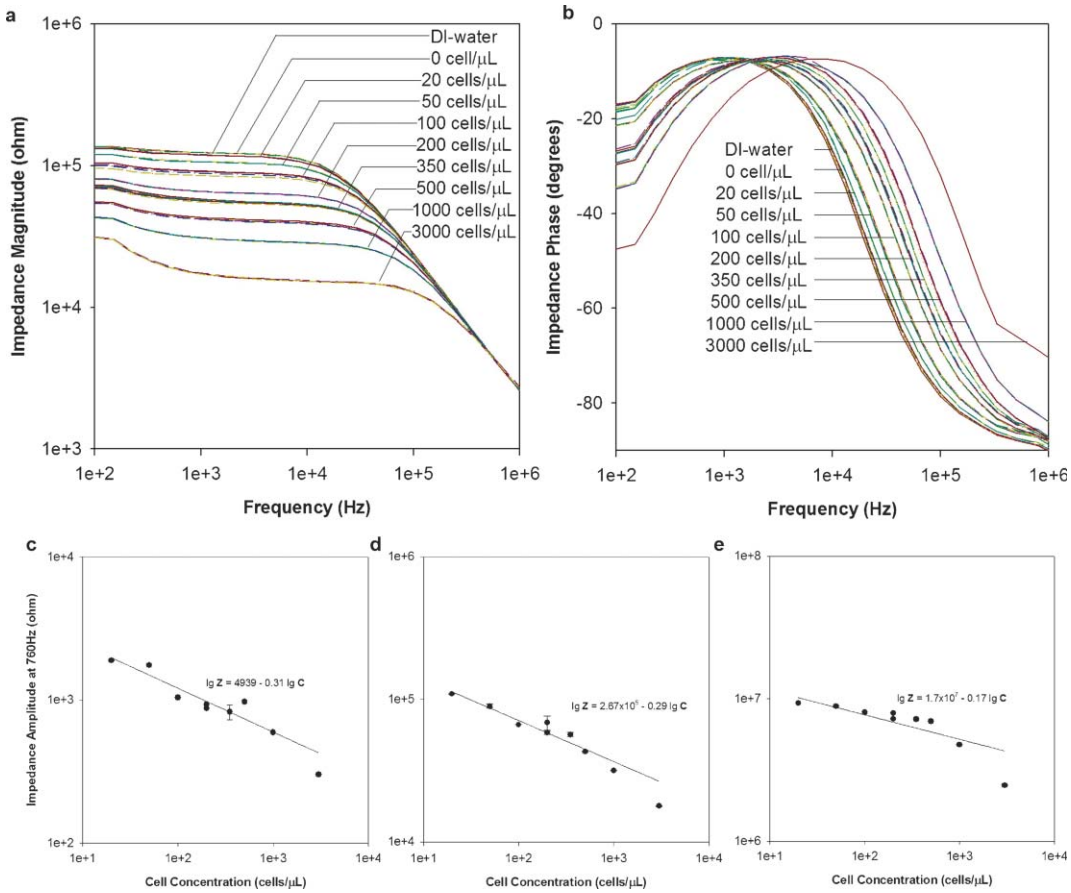

Fig. 2 Impedance spectra and impedance change as a function of cell concentration using cell lysate obtained off-chip. (a) Impedance magnitude and (b) phase spectra of DI water and cell lysate with different starting cell concentrations measured on the IDT device. Three to five scans were performed at each cell concentration in the frequency range between 100 and 10^6 Hz. Impedance magnitude measured at 760 Hz is plotted in log–log scale as a function of cell concentration using (c) top–bottom electrodes, (d) IDT electrodes and (e) two rail electrodes. The solid dots in (c)–(e) are experimental measurements and they were fit to two-parameter power equations. The least square fits are shown as solid lines and equations in the graph. Error bars indicate the standard deviation from 3–5 continuous measurements within a single device.

measurement frequency due to the maximum separation of impedance magnitude at this frequency for all three electrodes. The response of impedance magnitude to cell concentration is linear in a log–log scale plot, similar to the relationship between the resistance of a simple electrolyte solution and solute concentration in the range relevant to our study.[21] This indicates that the release of the ionic contents from cells and the subsequent conductance of the medium in which the cells are lysed is proportional to the number of cells. Moreover, using ion release to detect cells appears to be extremely sensitive, and can detect as few as twenty cells per microlitre in a low conductive solution.

Impedance modeling and parameter extraction

As cell ion release mainly contributes to bulk conductance change, we used the circuit model shown in Fig. 3a to fit both impedance magnitude and phase spectra using least square criteria in MATLAB, to extract bulk conductance values $G_{sol} = 1/R_{sol}$. By iterating each of the initial conditions in the model, the least square error between the model and the experimental data was minimized, to a value of 10^{-13} or less.[28,29] The fitting is then terminated and the parameters are extracted and recorded.

Fig. 3b and c show a typical fitting of the impedance magnitude and phase spectra using lysate from solutions containing 3000 cells μL^{-1}: close match between the measurements (crosses) and fitting curves (solid lines) indicates that the selected circuit model well predicts the experimental system.

After extracting bulk conductance from all spectra, we plotted bulk solution conductance as a function of cell concentration (solid circles in Fig. 3d–f). With all three electrode designs, solution conductance increases linearly with the number of cells contributing to ion concentration, confirming our hypothesis that ion release and solution conductance change are proportional to cell number. We also observed that R_{sol} values dominate impedance magnitude measurements in an intermediate frequency range between 100 to 10 kHz. This indicates that the bulk conductance can be estimated by measuring impedance magnitude at a single frequency using a simple hand-held setup, instead of an LCR meter.

Slopes of the conductance curves represent measurement sensitivity of each electrode design. We observed that top–bottom electrodes have the highest detection sensitivity ($9.18 \times 10^{-7}\ \Omega^{-1}$ (cells per $\mu L)^{-1}$), while the simple two-rail electrodes have the lowest sensitivity ($9.92 \times 10^{-11}\ \Omega^{-1}$ (cells per $\mu L)^{-1}$); the detection sensitivity of the IDT electrodes falls in between ($1.90 \times 10^{-8}\ \Omega^{-1}$ (cells per $\mu L)^{-1}$). For easy visualization of cells within the microfluidic devices as well as sensitive detection of cell ion release, we chose the IDT electrodes for further cell capture and on-chip lysis experiments.

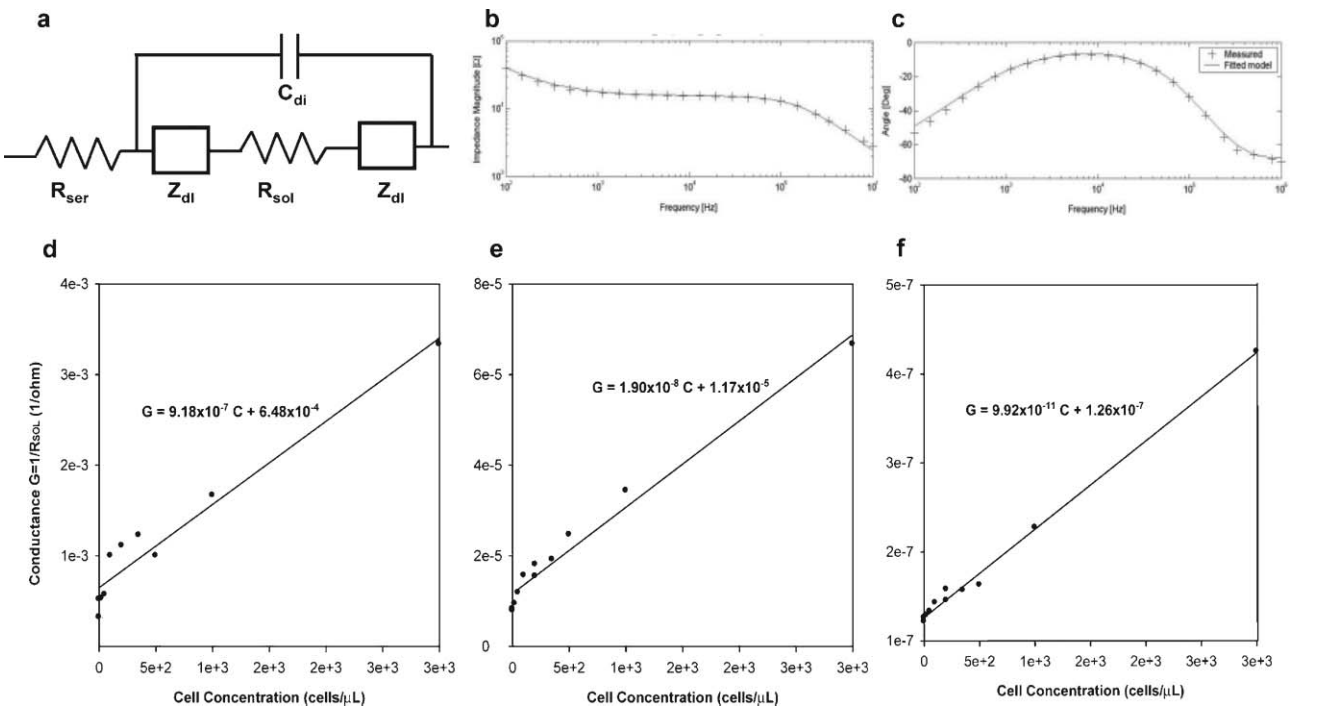

Fig. 3 Circuit model for fitting of the impedance spectra and extracted conductance as a function of cell concentration. (a) An equivalent circuit used in our study to model the electrode–electrolyte system for extracting bulk solution conductance, R_{sol}, which directly correlates with cell ion release. Representative fits of circuit to the complex impedance magnitude (b) and phase (c) spectra are plotted using off-chip cell lysate sample with a cell concentration of 3000 cells μL^{-1} in the IDT electrode chip. Crosses are the experimental data and solid lines show the fitting curves. From these fits, bulk conductance R_{sol} is extracted from spectra measured using (d) top–bottom electrodes, (e) IDT electrodes and (f) two-rail electrodes. Linear relationships between measured bulk solution conductance (solid dots) and cell concentration are observed using all electrode geometries and the best fit are shown as solid lines and equations in (d)–(f). Error bars in (d)–(f) indicates the standard deviation from 3–5 continuous measurements within a single device.

Optical characterization of on-chip cell lysis using hypotonic sugar solutions

After confirming the feasibility of detecting cells through their ion release using off-chip lysate and impedance spectroscopy, we were interested in testing this strategy to detect and quantify cells captured within microfluidic devices. To accomplish on-chip cell lysate impedance spectroscopy, we needed to first replace electrolyte-rich whole blood or saline buffer with a non-conductive, isotonic solution, to reduce background conductivity in the microfluidic channel and establish a baseline measurement. The off-chip experiments using DI water for cell lysis could not be applied directly to on-chip cell lysis, as cells suspended in DI water lyse immediately, and the lysate would be washed out of the chip prior to impedance measurements. Given the requirement that the medium into which the cells are lysed be as non-conductive as possible, and the need to wash away the ionic and protein content from the blood sample itself, we evaluated different low-conductive media as cell wash and cell stabilization solutions. We found that a sugar-based washing solution containing 8.5% sucrose and 0.3% dextrose satisfied the two criteria of ion removal and cell stabilization (data not shown). Impedance of this solution is close to deionized water, but cell viability can be maintained for more than 60 min.[30] Further dilutions of this solution with deionized water can be expected to decrease the solution osmolarity, so that lysing speed can be controlled by adjustments in the dilution factor.

To test lymphocyte viability and lysis in low-conductivity sugar solutions, we isolated CD4+ T lymphocytes from PBMCs within functionalized microchannels, as described.[8] After washing off unbound cells, we introduced the low-conductive 8.5% sucrose–0.3% dextrose washing solution, as well as more hypotonic sugar solutions. After flow of the sugar solution was stopped, the number of intact cells on the imaged area (600 mm × 800 mm) was counted every 30 s by fluorescence microscopy. Fig. 4 shows the percentage of viable cells *versus* time in the 8.5% sucrose–0.3% dextrose solution, and in different dilutions of this solution. Lymphocytes remain intact for at least 30 min in 8.5% sucrose–0.3% dextrose; lysis accelerates in more dilute sugar solutions. Based on these results, the 8.5% sucrose–0.3% dextrose solution was used as the initial wash solution, and a solution containing 2% sucrose and 0.07% dextrose was chosen for on-chip cell lysis. With this combination, we observed that up to 15% of captured cells lyse in the first minute of solution exchange, minimizing ion loss due to flow, while around 80% of cells are lysed within 10 min, making timely measurement possible.

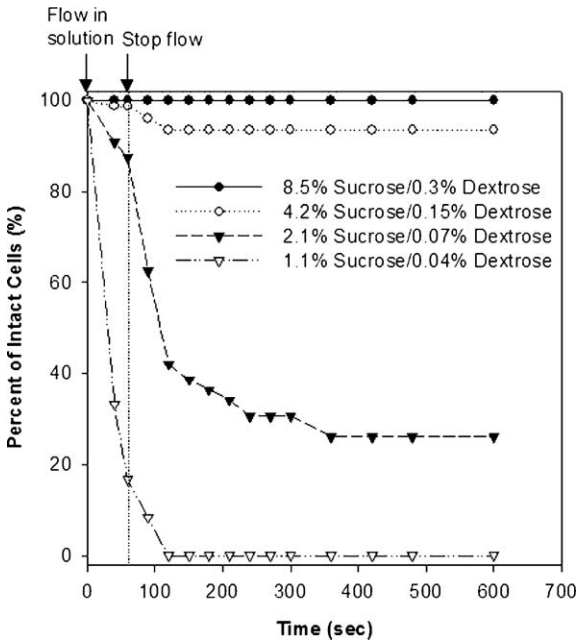

Fig. 4 Percentage of viable cells as a function of time in different concentrations of low conductivity sugar solution observed under a fluorescence microscope. CD4+ T cells were captured in antibody-immobilized devices, followed with flowing in sugar solutions of different concentrations at 10 mL min^{-1} for 2 min. After the solution flow was stopped, cells were incubated at room temperature in this solution for 8 min and the number of intact cells was counted under a fluorescent microscope every 30 s. The percentage of intact cells was calculated by dividing the number of intact cells by the total number of cells before injection of each sugar solution.

Impedance spectroscopy for on-chip cell lysis

After optimizing the ion-free, low conductive solutions for cell washing and lysis, we next measured impedance changes after on-chip cell capture and cell lysis. CD4+ T cells were captured from culture media, rinsed with PBS buffer, and rinsed again with the isotonic 8.5% sucrose–0.3% dextrose solution. After measurements of impedance baselines, the low conductivity cell lysing solution (2% sucrose–0.07% dextrose) was introduced into the microfluidic devices and cells were allowed to lyse for 10 min. Reference spectra were obtained with deionized water. Throughout the experiment, impedance spectra were acquired continuously. However, impedance measurements at a single frequency between 100 to 10 000 Hz reflected very well the changes of the solution's electrical property arising from cell lysis. For example, Fig. 5a shows the typical change of impedance magnitude acquired at the frequency of 760 Hz before and after on-chip cell lysis. Impedance magnitude remains in the low kΩ range when cells are in PBS, due to the high ionic concentration of saline buffers. Impedance increases dramatically to above ten kΩ upon introduction of the low-conductive 8.5% sucrose–0.3% dextrose washing solution. When cells are kept in the washing solution in a static state, impedance magnitude decreases slightly, likely due to low-level cell ion release in a hypo-osmotic environment. After injection of the ion-free 2% sucrose–0.07% dextrose lysing solution, we noticed an initial impedance jump. This was followed by an abrupt drop of impedance and a subsequent slower impedance decrease. This two-phase impedance drop during cell lysis matches the optical observation of cell lysis in the same solution (Fig. 4), suggesting that the decrease of impedance magnitude arises from lysis of the captured cells.

Following application of the fitting procedure described above, we extracted bulk conductance from the impedance spectra and the conductance change before and 10 min after introduction of the lysing solution. When we compare

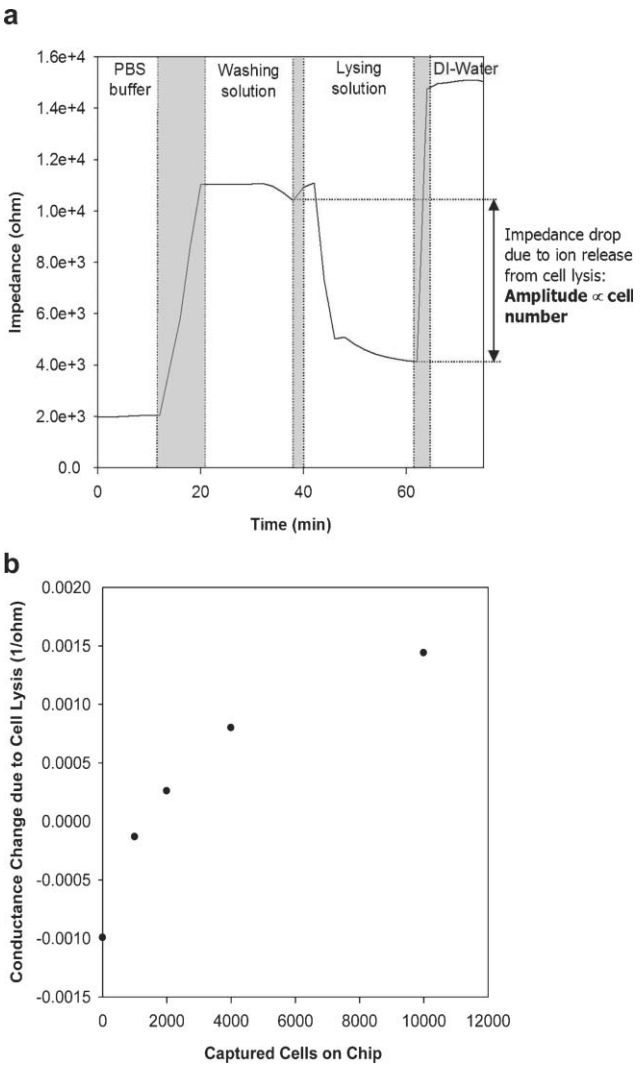

Fig. 5 Impedance measurement at 760 Hz and conductance change in the process of on-chip cell lysis. (a) Impedance magnitude at 760 Hz during the process of cell capture and on-chip lysis. The respective incubation steps are labelled on top of the graph and the shaded areas between these labelled steps are transient states during solution exchanges. The impedance drop before and 10 min after injecting the lysing solution is associated with cell lysis and is used as a cell-numbers indicator. (b) Conductance change *versus* the number of cells captured within microfluidic devices. Bulk solution conductance was extracted from the impedance spectra, and conductance drop before and 10 min after flowing in the lysing solution was taken as the indicator to count cells. This conductance change increases proportionally with the number of cells captured within the microfluidic chip, suggesting immobilized cells can be counted by electrical measurement of their ion release. Nonlinearity of the relationship may arise from incomplete diffusion of ions within the measurement time. Each data point in the plot represents a measurement from one device.

this conductance change to manual cell counts within the microfluidic devices (Fig. 5b), it is evident that bulk conductance changes are proportional to the number of captured cells contributing to ions. This successfully demonstrates that cells can be detected and counted within a microfluidic device through electrical measurement of the impedance and conductance of cell lysate.

Discussion

We describe here a method to detect and quantify immobilized cells in a microfluidic device through bulk electrical measurements based on cell ion release using impedance spectroscopy. We selected CD4+ T lymphocytes as the target cells for detection due to their clinical significance for the management of HIV infected patients.[31] The most immediate use of a microfluidic CD4 counter would be to differentiate the CD4 threshold of 200 cells μL^{-1} for treatment decisions.[32,33] The detection limit of cell lysate impedance spectroscopy clearly meets this requirement and shows promise in the development of microfluidic CD4 count diagnostic tools that can be used at the point-of-care. In addition, this cell counting strategy is not limited to the detection of blood cells, but can be applied to any biological target with rich ion content. To our knowledge, the capability to isolate and detect 1 cell on a millimetre square size area, or to detect 20 cells in a microlitre volume, represents the most sensitive approach to enumerate immobilized cells using a non-optical method.

Microchip devices used in the current study are composed of surface patterned microelectrodes fabricated within a microfluidic channel. The microchannel walls are functionalized with a monoclonal anti-CD4 antibody and the electrodes are passivated using BSA. The channel design and sample flow conditions are selected to ensure specific isolation of CD4+ T lymphocytes from whole blood with high efficiency, as described previously.[8] With appropriate electrode layout for on-chip cell lysis and counting (Fig. 1c), both isolation purity and yield remain above 90% from whole blood, due to maintenance of >85% of the affinity surface areas. Very few cells attach non-specifically on the electrode surfaces when observed under an optical microscope (data not shown), demonstrating expected device performance for cell isolation.

The separated cells are further detected by complete cell lysis and bulk conductance measurements using surface electrodes. As an effort to identify the frequency range that yields the best detection sensitivity, we acquired impedance magnitude and phase spectra as a function of frequency in this study, and fit the spectra to a circuit model to extract bulk conductance. With the knowledge of optimal frequency range (between 100 and 10 000 Hz in Fig. 2a) and the observation that R_{sol} values dominate impedance magnitude at these frequencies, one can estimate bulk conductance in seconds by monitoring impedance magnitude at a single frequency (*e.g.* 760 Hz) using a hand-held setup. Thus, the whole process from cell capture to cell lysis and detection could be accomplished in less than 10 min.

Specifically, for detection and monitoring of CD4 cells in HIV-infected patients, 200 cells μL^{-1} is used as a clinical decision point. We show here that integration of an immunoaffinity cell capture approach with an electrical detection method can meet this detection threshold. The microfluidic device we describe is capable of isolating specific cell types from blood and quantifying cell number, and can serve as a single-use cartridge for a hand-held instrument to provide simple, fast and affordable cell counting in point-of-care settings.

The ability to detect cells electrically, as opposed to optically, presents the following key advantages: (i) label-free detection, (ii) potential for automation, and amenability to the development of a small table top or hand-held instrument, (iii) potential for integration with microfluidic devices; and (iv) sensitivity of detection in a physiologically and clinically relevant range of cell concentrations. Compared to other electrical approaches to counting cells, cell lysate impedance spectroscopy demonstrates a few orders of magnitude improvement in detection sensitivity. This is due to the reduced background conductance when cells are stabilized in an ion-free, low conductivity sugar solution and rich ion content released from mammalian cells upon hypotonic lysis. Changes in solution conductance in the process of cell lysis are extracted from the spectra of impedance measurements. We demonstrate that bulk conductance of cell lysate is proportional to the original cell number, which forms the basis of cell lysate impedance spectroscopy. This method is sensitive enough to detect as low as twenty cells per microlitre in a device with a volume of 10 μL and a footprint of 2 cm^2, which represents $<10^{-4}$ volume replacement and 10^{-4} surface coverage.

To measure bulk conductance in a microfluidic device, we patterned surface electrodes within microchannels and modeled impedance spectra using a simple circuit, which contains a dielectric capacitance (C_{di}) in parallel with the sum of bulk solution resistance (R_{sol}) and interfacial impedance (Z_{dl}). From experimental fitting, we observe that the magnitude of Z_{dl} is generally much smaller than the solution resistance R_{sol}. As a result, R_{sol} dominates the circuit at the low frequency range (<1–10 kHz depending on electrode geometry), leading to relatively constant impedance, independent of frequency change. Dominance of R_{sol} in the low frequency range is also observed as humps in the phase spectra. As the ionic concentration of the solution increases, bulk solution resistance decreases, shifting the range where R_{sol} dominates to higher frequencies, and decreasing the overall impedance in that same range. In the high frequency range (10–100 kHz), on the other hand, the dielectric capacitor (C_{di}) dominates, resulting in an impedance magnitude drop with frequency increase. At even higher frequencies (>100 kHz), inductance of the electrochemical device and connecting wires all contribute to the impedance spectra, resulting in merging of all the impedance curves regardless of solution conductivity.[34]

Monitoring biological ion release using impedance spectroscopy in a microdevice is a well established technique to study metabolism and growth of microorganisms.[23,24] However, similar approaches have not been reported previously for mammalian cells, likely due to their intolerance to an ion-free environment, which is required to reduce background conductance for the sensitive measurement of ions released by cells. We demonstrate here the possibility to maintain the viability of primary cells in an ion-free sugar solution and the feasibility to measure bulk conductance change due to cell ion release through impedance spectroscopy. This strategy differs in principle from other non-optical strategies to detect adherent cells, such as surface impedance spectroscopy, field effect sensors and mechanical cantilevers.[15,18,35–38] These approaches are based on detecting differences between the electrical or physical properties of cells and the surrounding medium. This difference is generally small; thus the characteristic sensing elements and the target entity are usually of comparable dimensions for sensitive detection, unless the differences are manually enhanced.[39,40] In contrast, in our approach, the electrical signal is amplified by taking advantage of the large amount of ions pre-existing inside the target cells. This allows for sensitive detection of cells with very low surface coverage or volume replacement, without significant additional manipulation.

Another advantage of our strategy is the flexibility in sensor design. The possibility to sensitively measure bulk impedance using simple two rail, co-planar electrodes or top–bottom electrodes indicate one could use simple metal plates or wires to implement our approach with less sophisticated technologies without sacrificing the detection limit. When the three electrode geometries are compared, the top–bottom electrodes demonstrated the highest detection sensitivity, while simple two rail electrodes have the lowest detection sensitivity. Assuming the solution in the fluidic channel is a simple conductor, theoretical conductance measured at each condition can be calculated using the following equation:

$$G = \sigma mA/L \quad (2)$$

where σ is the solution conductivity, A is the solution cross-sectional areas between the electrodes, L is the spacing between electrodes and m is the electrode repeats. Since solution conductivity is independent of the device design, this geometrical factor essentially determines measurement sensitivity. When the geometrical factor (mA/L) is calculated for the three electrode designs used in this study, we obtain values of 400, 150 and 0.065 cm for the top–bottom, IDT and simple electrodes, respectively. This order of geometrical factor matches our measurement sensitivity from the conductance plots (Fig. 3d–f). However, when we calculate theoretical conductance using eqn (2) by assuming each cell releases 10^{-14} molar ions after complete lysis, the predicted conductance is one to three orders of magnitude higher than measurements obtained using off-chip lysate, indicating ions in the bulk don't contribute to conduction to the same level. In fact, DeSilva *et al.* have hypothesized that electrical conductance through in-plane electrode islands bridged with immobilized proteins was dominated by ion conduction of hydrated protein layers.[41] Applying their model to our system, the dominating conductive layer could be close to the substrate and is much thinner than the channel dimensions, explaining the deviation between measurements and calculated conductance using eqn (2). When the impedance magnitude is compared between on-chip and off-chip lysing experiments using IDT electrodes, we also observed an order of magnitude difference. This difference may be accounted for by separate preparations of these two types of devices: devices used for the off-chip lysate experiments were not subjected to surface modification, while those for on-chip lysis contained multiple layers of chemicals and proteins in the gap between the electrodes, changing the electrical properties of the gaps. In addition, electrodes used for on-chip lysis experiments are primed with albumin, which is likely to alter electron transfer

kinetics and ion diffusion characteristics on the electrode.[34] Despite the difference in absolute impedance magnitude between these two types of devices, measurements taken using devices under the same preparation clearly demonstrate comparable performance, as observed with reference solution spectra.

An interesting observation noted is the slight impedance drop when keeping cells in the low-conductive washing solution. This may indicate the release of ions from captured cells despite an intact morphology under optical microscopy. As the washing solution is slightly hypo-osmotic (270 mOsm), cells are likely to swell when they are first exposed to the washing solution. Transient osmotic swelling and the following regulatory volume decrease (RVD) are known to cause KCl efflux induced by parallel activation of K^+ and Cl^- channels,[42–45] which can result in the observed solution conductance decrease. This observation suggests the possibility to directly study cell response to a hypotonic solution and RVD using electrical approaches. Such measurements could provide better sensitivity compared to conventional methods based on optical measurements of cell sizes, which have low throughput and are prone to measurement errors. Cell ion release and volume adjustment in response to changes in environmental osmolarity may also explain the heterogeneous cell lysis as observed in Fig. 4. Since memory and native T cells have been reported to contain different ion stores,[46] it is not surprising that these cells may have a different capability to adjust to hypo-osmotic conditions, and demonstrate different lysing speed. However, phenotyping fast and slow lysing lymphocyte populations in a hypotonic solution is beyond the scope of this paper and will be examined in a later study.

Conclusions

In conclusion, we demonstrate in this paper an electrical method of high sensitivity that allows the detection of a small number of immobilized cells in microfluidic devices. This method utilizes impedance spectroscopy to probe bulk solution conductance change associated with cell ion release. Using this method, we show that bulk conductance is proportional to the number of cells contributing to ion content in the solution, and the detection sensitivity can go down to 20 cells μL^{-1}. The conductance information can be potentially obtained by impedance measurements at a single frequency of 760 Hz with a simple setup. This method is compatible with very simple electrode designs and may serve as an important technology for automated hand-held cell counters for point-of-care diagnostics.

Acknowledgements

We would like to acknowledge D. Maish at Purdue University for drawing blood from volunteers for preparation of buffy coat, Ms Lisa Reece and Prof. James Leary at Purdue University for training Y. Liu in buffy coat preparation, and Prof. Demir Akin for valuable discussions. We would also like to thank the support of the staff in the Birck Nanotechnology Center at Purdue University. We are also very grateful for the technical support from Mr Octavio Hurtado at the BioMEMS Resource Center and Mr Donald Poulsen at Shriners Hospital. This work was partially supported by the National Institute of Biomedical Imaging and Bioengineering under Grant No. P41 EB002503 (BioMEMS Resource Center), which also hosted R. Bashir's sabbatical at the BioMEMS Resource Center in 2006–2007.

References

1 J. H. Qin, N. N. Ye, X. Liu and B. C. Lin, *Electrophoresis*, 2005, **26**, 3780–3788.
2 C. Q. Yi, C. W. Li, S. L. Ji and M. S. Yang, *Anal. Chim. Acta*, 2006, **560**, 1–23.
3 H. Andersson and A. van den Berg, *Sens. Actuators, B*, 2003, **92**, 315–325.
4 M. B. Fox, D. C. Esveld, A. Valero, R. Luttge, H. C. Mastwijk, P. V. Bartels, A. van den Berg and R. M. Boom, *Anal. Bioanal. Chem.*, 2006, **385**, 474–485.
5 H. Andersson and A. van den Berg, *Lab Chip*, 2004, **4**, 98–103.
6 P. Gascoyne, J. Satayavivad and M. Ruchirawat, *Acta Trop.*, 2004, **89**, 357–369.
7 R. Gambari, M. Borgatti, L. Altomare, N. Manaresi, G. Medoro, A. Romani, M. Tartagni and R. Guerrieri, *Technol. Cancer Res. Treat.*, 2003, **2**, 31–39.
8 X. Cheng, D. Irimia, M. Dixon, K. Sekine, U. Demirci, L. Zamir, R. G. Tompkins, W. Rodriguez and T. Mehmet, *Lab Chip*, 2007, **7**, 170–178.
9 M. Toner and D. Irimia, *Annu. Rev. Biomed. Eng.*, 2005, **7**, 77–103.
10 B. H. Weigl, R. L. Bardell and C. R. Cabrera, *Adv. Drug Delivery Rev.*, 2003, **55**, 349–377.
11 J. Kruger, K. Singh, A. O'Neill, C. Jackson, A. Morrison and P. O'Brien, *J. Micromech. Microeng.*, 2002, **12**, 486–494.
12 M. A. McClain, C. T. Culbertson, S. C. Jacobson and J. M. Ramsey, *Anal. Chem.*, 2001, **73**, 5334–5338.
13 S. Gawad, L. Schild and P. Renaud, *Lab Chip*, 2001, **1**, 76–82.
14 D. Huh, Y. C. Tung, H. H. Wei, J. B. Grotberg, S. J. Skerlos, K. Kurabayashi and S. Takayama, *Biomed. Microdev.*, 2002, **4**, 141–149.
15 M. Koch, A. G. R. Evans and A. Brunnschweiler, *J. Micromech. Microeng.*, 1999, **9**, 159–161.
16 M. C. Lundien, K. A. Mohammed, N. Nasreen, R. S. Tepper, J. A. Hardwick, K. L. Sanders, R. D. Van Horn and V. B. Antony, *J. Clin. Immunol.*, 2002, **22**, 144–152.
17 I. Giaever and C. R. Keese, *Proc. Natl. Acad. Sci. U. S. A.*, 1984, **81**, 3761–3764.
18 R. Ehret, W. Baumann, M. Brischwein, A. Schwinde, K. Stegbauer and B. Wolf, *Biosens. Bioelectron.*, 1997, **12**, 29–41.
19 D. J. Aidley and P. R. Stanfield, *Ion Channels: Molecules in Action*, Cambridge University Press, Cambridge, UK, 1996.
20 *Electrochemical Aspects of Ionic Liquids*, ed. H. Ohno, Wiley–Interscience, Hoboken, NJ, 2005.
21 Omega Engineering, Technical Conductivity and Resistivity, accessed: December 30, 2006.
22 J. M. Lee, M. S. Jhon and H. Eyring, *Proc. Natl. Acad. Sci. U. S. A.*, 1979, **76**, 5421–5423.
23 R. Gomez-Sjoberg, D. T. Morisette and R. Bashir, *J. Microelectromech. Syst.*, 2005, **14**, 829–838.
24 R. Gomez, R. Bashir and A. K. Bhunia, *Sens. Actuators, B*, 2002, **86**, 198–208.
25 A. Ferrante and Y. H. Thong, *J. Immunol. Methods*, 1980, **36**, 109–117.
26 D. English and B. R. Andersen, *J. Immunol. Methods*, 1974, **5**, 249–252.
27 S. Pfau, D. Leitenberg, H. Rinder, B. R. Smith, R. Pardi and J. R. Bender, *J. Cell Biol.*, 1995, **128**, 969–978.
28 K. J. Vetter, *Electrochemical kinetics : theoretical and experimental aspects*, Academic Press, New York, 1967.
29 *Impedance spectroscopy : theory, experiment, and applications*, ed. Evgenij Barsoukov, J. R. Macdonald, Wiley–Interscience, Hoboken, N. J., 2005.
30 P. Y. Chiou, A. T. Ohta and M. C. Wu, *Nature*, 2005, **436**, 370–372.

31 Department of Health and Human Services (October 6, 2005) Guidelines for the Use of Antiretroviral Agents in HIV-1-Infected Adults and Adolescents, http://aidsinfo.nih.gov/ContentFiles/AdultandAdolescentGL.pdf, accessed 20 March 2006.
32 Centers for Disease Control and Prevention Revised classification for HIV infection and expanded surveillance case definition for AIDS among adolescents and adults, in *MMWR Morbidity and Mortality Weekly Report* 1–19, 1992.
33 World Health Organization (4 November 2005) Patient Monitoring Guidelines for HIV Care and ART, http://www.who.int/hiv/pub/guidelines/patientmonitoring.pdf, accessed 20 March 2006.
34 E. Katz and I. Willner, *Electroanalysis*, 2003, **15**, 913–947.
35 P. Fromherz, A. Offenhausser, T. Vetter and J. Weis, *Science*, 1991, **252**, 1290–1293.
36 B. S. Bull, Schneide Ma and G. Brecher, *Am. J. Clin. Pathol.*, 1965, **44**, 678.
37 C. Tiruppathi, A. B. Malik, P. J. Delvecchio, C. R. Keese and I. Giaever, *Proc. Natl. Acad. Sci. U. S. A.*, 1992, **89**, 7919–7923.
38 I. Giaever and C. R. Keese, *Proc. Natl. Acad. Sci. U. S. A.*, 1991, **88**, 7896–7900.
39 E. Katz, I. Willner and J. Wang, *Electroanalysis*, 2004, **16**, 19–44.
40 J. Wang, *Anal. Chim. Acta*, 2003, **500**, 247–257.
41 M. S. Desilva, Y. Zhang, P. J. Hesketh, G. J. Maclay, S. M. Gendel and J. R. Stetter, *Biosens. Bioelectron.*, 1995, **10**, 675–682.
42 S. F. Pedersen, E. K. Hoffmann and J. W. Mills, *Comp. Biochem. Physiol., A: Physiol.*, 2001, **130**, 385–399.
43 Y. Okada, E. Maeno, T. Shimizu, K. Dezaki, J. Wang and S. Morishima, *J. Physiol.*, 2001, **532**, 3–16.
44 H. Pasantes-Morales, V. Cardin and K. Tuz, *Neurochem. Res.*, 2000, **25**, 1301–1314.
45 G. T. Charras, J. C. Yarrow, M. A. Horton, L. Mahadevan and T. J. Mitchison, *Nature*, 2005, **435**, 365–369.
46 A. Sigova, E. Dedkova, V. Zinchenko and I. Litvinov, *FEBS Lett.*, 1999, **447**, 34–38.